PROGRESSIVE FAILURE METHODOLOGIES FOR PREDICTING RESIDUAL STRENGTH AND LIFE OF LAMINATED COMPOSITES

Charles E. Harris[1]
David H. Allen[2]
T. Kevin O'Brien[3]

ABSTRACT

This paper describes two progressive failure methodologies currently under development by the Mechanics of Materials Branch at NASA Langley Research Center. The "damage tolerance/fail safety methodology" developed by O'Brien is an engineering approach to ensuring adequate durability and damage tolerance by treating only delamination onset and the subsequent delamination accumulation through the laminate thickness. The "continuum damage model" developed by Allen and Harris employs continuum damage mechanics concepts and uses loading history dependent damage growth laws to predict laminate strength and life. The philosophy, mechanics framework, and current implementation status of each methodology are presented in the paper.

INTRODUCTION

The next generation commercial transport aircraft are likely to have a significant amount of primary airframe structure fabricated of advanced composite materials with graphite fiber reinforcement in an organic matrix. The damage tolerance characteristics of composite materials are fundamentally different from monolithic metallic materials and, therefore, cannot be predicted by current metals-based methods. For example, composite structures are not susceptible to the development of dominant macro-cracks through the fatigue growth of micro-cracks as are metallic structures. Therefore, there is no single parameter such as the stress intensity factor that can be used to predict crack growth and the subsequent residual strength of a composite structure. However, microcracking frequently develops in a progressive fashion leading to laminate failure. Zones of damage (sublaminate cracking) may develop in high strain gradient fields produced by geometric discontinuities and may also be produced by foreign object impacts. These zones of damage may consist of intraply matrix cracks, local fiber fracture, and interply delaminations. The individual damage mechanisms are often interactive with one mode of damage being the initiator of a second mode of damage. At the local level, these zones of damage will result in the failure of the principal load-carrying plies which will eventually

---

[1]Head, Mechanics of Materials Branch, NASA Langley Research Center
[2]Professor, Aerospace Engineering Department, Texas A&M University
[3]Senior Scientist, U.S. Army Aerostructures Directorate, NASA Langley Research Center

precipitate global structural failure. Additionally, the local damage development will also effect the global structural response through changes in the local stiffness properties which will alter the structural load paths. Therefore, an iterative analysis procedure between the global and local levels is required to rigorously predict progressive damage development leading to structural failure.

Two progressive failure methodologies are being independently developed in the Mechanics of Materials Branch at NASA Langley Research Center. While considerable synergism exits between the two efforts, the two models are being developed from quite different mechanics philosophies. The damage tolerance/fail safety methodology developed by O'Brien is an engineering approach to ensuring adequate durability and damage tolerance by treating only delamination onset and the subsequent delamination accumulation through the laminate thickness. On the other hand, the continuum damage model developed by Allen and Harris employs continuum damage mechanics concepts and uses loading history dependent damage growth laws to predict laminate strength and life. This paper will review the mechanics formulation of each methodology and will discuss recent advances in using the methods to analyze relevant structural geometries.

The purposes of this paper are to establish the philosophy guiding the development of each methodology, to review the model formulations, and to establish the current progress toward structural analysis implementation. It is well beyond the scope of this paper to present all of the mathematical details associated with the two subject methodologies. The details of the mathematical formulations have been previously published by the authors and references to these publications are cited throughout this paper. The interested reader is strongly encouraged to review the references and contact the authors for further details or to discuss issues for clarification.

PART I: DAMAGE THRESHOLD/FAIL SAFETY APPROACH

Many papers have been published recently where the rate of delamination growth with fatigue cycles, da/dN, has been expressed as a power law relationship in terms of the strain energy release rate, G, associated with delamination growth [1-4]. This fracture mechanics characterization of delamination growth in composites is analagous to that of fatigue crack growth in metallic structures, where the rate of crack growth with cycles is correlated with the stress intensity factor at the crack tip. However, delamination growth in composites occurs too rapidly over a fairly small range of load to be incorporated into a classical damage tolerance analysis for fail safety [2,5,6]. While in metals the range of fatigue crack growth may be described over as much as two orders of magnitude in G, the growth rate for a delamination in a composite is often characterized over barely one order of magnitude in G. Hence, small uncertainties in the applied load may yield large (order of magnitude) uncertainties in delamination growth.

Different damage mechanisms may also interact with the delamination and increase the resistance to delamination growth. Delamination growth resistance curves may be generated to characterize the retardation in delamination growth from other mechanisms [7-9]. These delamination resistance curves are analogous to the R-curves generated for ductile metals that account for stable crack growth resulting from extensive

plasticity at the crack tip. However, unlike crack-tip plasticity, other composite damage mechanisms, such as fiber bridging and matrix cracking, do not always retard delamination growth to the same degree. Hence, the generic value of such a characterization is questionable.

One alternative to using the classical damage tolerance approach for composites as it is used for metals would be to use a strain energy release rate threshold for no delamination growth and design to levels below this threshold for infinite life. Composites materials are macroscopically heterogeneous, with stiffness discontinuities that give rise to stress singularities at known locations, such as straight edges, internal ply drops, and matrix cracks. Although these singularities are not the classical $r^{-1/2}$ variety observed at crack tips, and hence cannot be characterized with a single common stress intensity factor, they can be characterized in terms of the strain energy release rate, G, associated with the eventual delamination growth.

The most common technique for characterizing delamination onset in composite materials is to run cyclic tests on composite specimens, where G for delamination growth is known, at maximum load or strain levels below that required to create a delamination under quasi-static loading. A strain energy release rate threshold curve for delamination onset may be developed by running tests at several maximum cyclic load levels and plotting the cycles to delamination onset versus the maximum cyclic G, corresponding to the maximum cyclic load or strain applied [10-14]. This G threshold curve may then be used to predict delamination onset in other laminates of the same material, or from other sources in the same laminate [10-15].

One concern with a no-growth threshold design criteria for infinite life has been the uncertainty inherent in predicting service loads. If service loads are greater than anticipated, then corresponding G values may exceed no-growth thresholds and result in catastrophic propagation. This concern is paramount for military aircraft and rotorcraft, where original mission profiles used to establish design loads are often exceeded once the aircraft is placed in service. However, unlike crack growth in metals, catastrophic delamination growth does not necessarily equate to structural failure. In situations where the structure experiences predominantly tensile loads, such as composite rotor hubs and blades, delaminated composites may have inherent redundant load paths that prevent failure and provide a degree of fail safety [5]. This degree of fail safety has led some designers to think of composite delamination as a benign failure mode. Unfortunately, delaminations may occur at several locations in a given component or structure. Delaminations will typically initiate at edges, holes, ply drops, and ultimately, matrix cracks. Hence, a composite mechanics analysis that considers each of these potential sites must be performed to ensure that the structure is fail safe. Previously, a damage-threshold/fail-safety approach for composite fatigue analysis was proposed [5] that involved the following steps:

1. Predict delamination onset thresholds using fracture mechanics.

2. Assume delamination threshold exceedence corresponds to complete propagation.

3. Determine the remaining load-carrying capability of the composite with delamination present using composite mechanics (i.e., check for fail safety).

4. Iterate on Steps 1 to 3 to account for multiple sources of delamination.

This type of analysis need only be applied to primary structures. However, Step 1 may be used to demonstrate the delamination durability of any composite structure, thereby providing an assessment of component repair or replacement costs over anticipated structural service lives. Step 2 reflects a conservative way to deal with the rapid delamination growth rates observed relative to metals as discussed earlier. An alternative to Step 2 would be to predict delamination growth rates using growth laws that incorporate *R*-curve characterizations, thereby taking into account the resistance provided by other damage mechanisms. Such a characterization has been attempted previously [9], but should be used with caution because it is not truly generic. A third approach for Step 2 is to monitor stiffness loss in real time, and hence reflect the consequence of delamination growth, and other damage mechanisms, as they occur. However, in most structural applications, real-time monitoring of stiffness loss may not be practical, so the conservative approach outlined in Step 2 would be applied. Finally, Step 3 acknowledges that the residual strength of the composite is a function of laminate structural variables (such as layup, stacking sequence, and ply thickness), and it is not uniquely a question of material characterization. Hence, the damage-threshold/fail-safety concept offers both the benefits of generic material characterization using fracture mechanics, while reflecting the unique structural character of laminated composite materials.

Tension Fatigue Life Prediction: A Case Study

The damage-threshold/fail-safety approach was used to predict the tension fatigue life of graphite/epoxy, glass/epoxy, and glass/graphite/epoxy hybrid laminates [16]. First, delamination onset behavior for the glass/epoxy and graphite/epoxy materials in fatigue was characterized in terms of the strain energy release rate using edge delamination onset fatigue data. Then, stiffness loss associated with damage onset and growth was measured. Next, the influence of local delaminations from matrix cracks on the strain in the load-bearing zero degree plies was quantified. The onset of local delaminations through the laminate thickness was predicted using a strain energy release rate solution for local delamination. Finally, fatigue life was determined by predicting the accumulation of these local delaminations through the thickness, calculating their effect on the strain in the zero degree plies, and comparing this local strain to the increase in global strain due to stiffness loss associated with damage.

Delamination Onset Characterization

Delamination onset behavior for the glass/epoxy and graphite/epoxy materials in fatigue was characterized in terms of the strain energy release rate using edge delamination onset fatigue data. Fig. 1 compares fatigue delamination onset criteria for E-glass/epoxy and graphite/epoxy laminates with the same epoxy matrix. The lines shown in Fig.1 are fit through the lowest data point for quasi-static and cyclic loading, and hence, represent a lower bound characterization of delamination onset. Linear plots of the

maximum cyclic G versus log N, the number of cycles to delamination onset, were generated yielding a linear delamination onset criteria in the form

$$G = m \, logN + G_c \qquad (1)$$

where G_c and m are material parameters. The slope, m, was the same for both materials; however, the static G_c values were lower for the glass/epoxy because the glass/epoxy laminates failed in the fiber matrix interface.

Stiffness Loss

In order to predict stiffness loss as a function of fatigue cycles, the onset and growth of damage must be characterized in terms of a generic parameter that is representative of the composite material being tested, but is independent of laminate structural variables such as lay-up, stacking sequence, and ply thickness. For delamination, this characterization is typically achieved using the strain energy release rate. For example, Fig. 2 shows the steps that would be required to predict stiffness loss associated with delamination as a function of fatigue cycles using a G characterization of delamination onset and growth. First, plots of the maximum cyclic G versus log N must be generated to characterize the onset of delamination [5,6,12,15] and power law relationships between G_{max} and the rate of growth of delamination with fatigue cycles are needed to characterize damage growth [1-4,6] (Fig. 2a). Using these material characterizations, the increase in delamination size, a, with fatigue cycles may be predicted (Fig. 2b). This information, in turn, may be used to predict the decrease in modulus with cycles associated with delamination, which, when combined with the stiffness loss due to other mechanisms that may be present (such as matrix plasticity and matrix cracking) yields the increase in global strain with cycles for a constant cyclic stress amplitude test (Fig. 2c).

Although the steps outlined above are straightforward, application of this procedure is complicated by the interaction between matrix crack formation and delamination growth, making it difficult to achieve a generic characterization of either one alone [17]. Therefore, instead of trying to predict stiffness loss as outlined in Fig. 2, stiffness loss was monitored experimentally. However, regardless of whether stiffness loss is measured or predicted, knowledge of the increase in global strain with cycles resulting from a loss in stiffness as damage accumulates is necessary, but not sufficient, to predict fatigue life. The final failure of the laminate is governed not only by loss in stiffness but also by the local strain concentrations that develop in the primary load-bearing plies (which in most laminates are zero-degree plies) as local delaminations originating at matrix ply cracks accumulate through the laminate thickness.

Strain Concentrations in Zero Degree Plies

Figure 3a shows that fatigue failures typically occur after the global strain has increased because of the fatigue damage growth, but before this global strain reaches the global strain at failure ε_F, measured during a static strength test [11,15,18,19]. Therefore, local strain concentrations must be present in the zero-degree plies that control the laminate strength. Once delaminations initiate at matrix ply cracks anywhere through the

laminate thickness, the local strain will increase significantly throughout the remaining through-thickness cross section [5,11,16,18-21]. These local strain concentrations may be calculated simply as

$$K_\varepsilon = E_{LAM}t_{LAM} / E_{LD}t_{LD}$$ (2)

where E and t are the moduli and thickness, respectively, of the original laminate (LAM) and the locally delaminated region (LD) which consists of the original laminate minus the cracked off-axis plies. These local strain increases may not have an immediate influence on the global strain measurement because delaminations starting from matrix cracks grow very little once they form. However, enough of them will eventually form to have some contribution to the global stiffness loss. The local strain concentration in the zero degree plies, however, is present as soon as the local delamination forms. If several delaminations form at matrix cracks throughout the laminate thickness at one location, then the local strain on the zero-degree plies at that location may reach the static failure strain, resulting in fatigue failure (Fig. 3b).

Each time a delamination initiates from a matrix crack, the local strain in the remaining through-thickness cross section, and hence in the zero-degree plies, increases to an amount equal to K_ε times the global cyclic strain, ε_{max}, until it reaches the static failure strain, ε_F, (Fig. 4a). A simpler way to visualize this process, however, is to reduce the static failure strain to some effective global ε_F value each time a new local delamination forms through the thickness. Hence, the effective ε_F would be equal to $\varepsilon_F/K_\varepsilon$. As local delaminations accumulate through the thickness, the effective ε_F would decrease incrementally. Meanwhile, the global strain would be rising due to stiffness loss associated with damage. Fatigue failure would correspond to the number of cycles where the damage growth increased the global maximum cyclic strain, ε_{max}, to the current value of the effective ε_F (Fig. 4b). This approach does not require a prediction of damage growth with fatigue cycles if the laminate stiffness loss, and hence the increase in global strain, can be monitored in real time. When this is possible, only the incremental decreases in the effective ε_F associated with local delamination accumulation through the thickness need to be predicted to determine fatigue life.

Local Delamination Onset Prediction

The number of fatigue cycles to onset of each local delamination through the thickness was predicted by using the linear delamination onset criteria with the strain energy release rate for the locally delaminated region (Fig.5) [16]. As shown in Fig.5, the thickness and modulus terms in the G equation for local delamination change for each successive local delamination that forms through the thickness. Therefore, as local delaminations accumulate through the thickness under a constant σ_{max}, the driving force (i.e., G) for each new delamination changes. Hence, fatigue life prediction for composite laminates requires a "cumulative damage" calculation, even for constant amplitude loading.

For the hybrid laminates [17], the number of cycles required for onset of local delaminations between two graphite/epoxy plies was predicted using G_C and m values for graphite/epoxy. The number of cycles required for onset of local delaminations that occurred between two glass/epoxy plies, or between adjacent glass/epoxy and graphite/epoxy plies, was predicted using the G_C and m values for glass/epoxy. As each local delamination formed through the laminate thickness, the reduction in the effective failure strain of the zero degree plies was calculated as outlined in the previous section.

Fatigue Life Determination

As previously mentioned, fatigue failure was assumed to occur when the increased global strain in the laminate, determined from measured stiffness loss, reached the reduced effective failure strain in the zero degree plies, resulting from the accumulation of local delaminations through the laminate thickness (Fig.4b). However, because of the scatter in the experimental data due to the variation in laminate modulus (i.e., the variation in ε_{max}) and the variation in static failure strain from specimen to specimen, a range of fatigue lives was determined for each stress level rather than a single value of life (Fig. 6). Figure 7 shows the fatigue life determination for [45/ -45/0]$_s$ hybrid laminates. The agreement between measured and calculated fatigue lives was very good, although calculated values were somewhat conservative at the higher cyclic loads.

In this tension fatigue case study, as each local delamination formed, ε_F was reduced by the appropriate K_ε to obtain an effective ε_F that was compared with the current value of ε_{max}, based on measured stiffness loss, to determine if fatigue failure had occurred. Hence, the ability to predict local delamination onset, and its effect on ε_F, facilitates the use of measured stiffness loss to determine fatigue life. However, for many composite structures, real-time stiffness measurement may not be practical. In these cases, the conservative approach for Step 2 in the damage-threshold/fail-safety approach outlined earlier could be applied. If the conservative approach was used to predict the tension fatigue life of [45/ -45/0/90]$_s$ laminates, for example, stiffness would decrease incrementally, i.e., ε_{max} would increase incrementally, with the onset of each damage mechanism. Figure 8 shows a sketch for conservative fatigue life prediction in [45/ -45/0/90]$_s$ graphite/epoxy and glass/epoxy laminates. Because matrix cracks can develop under static loading, ε_{max} is increased in the first load cycle, corresponding to the stiffness loss associated with saturation crack spacing in the off-axis plies. This stiffness loss would be greater for glass/epoxy laminates than for graphite/epoxy laminates [15]. When edge delamination occurs in the 0/90 interfaces, ε_{max} will increase again, corresponding to complete delamination across the laminate width. This stiffness loss would be greater for graphite/epoxy laminates than for glass/epoxy laminates [15]. However, ε_F would not change because edge delaminations do not create local strain concentrations in the zero-plies [16]. As each local delamination forms, the effective ε_F will decrease incrementally

based on the appropriate K_ε, and ε_{max} will increase incrementally, corresponding to delamination growth throughout the particular interface. When enough local delaminations form through the thickness such that $(\varepsilon_{max})_i \geq (\varepsilon_F)_i$, fatigue failure will occur.

Damage-Threshold/Fail-Safety Approach for Compression and Low-Velocity Impact

In the previous case study, and in the examples cited in Ref 5, the damage-threshold/fail-safety approach was illustrated for problems that involved only tension loading. However, this same approach may be applied to laminates subjected to compression loading. Delamination onset characterization would be conducted in the same way, with only the assessment of fail safety (Step 3) changing significantly.

The significance of accumulated delaminations on compression strength has been documented previously by comparing the strength of graphite epoxy [45/-45/90/0/45/-45/0₂/45/-45/0₂]s wing skin laminates with one, two, or three implanted delaminations through the thickness to identical laminates with either barely visible or visible impact damage (Fig. 9) [22]. These results show that the compression strength for laminates with 5.08 cm (2.0 in.) diameter implanted delaminations, normalized by the compression strength for the same laminates with a 6.33-mm (l/4-in.) open hole, decreases as the number of delaminations increases through the thickness. Still lower compression strengths were observed for the impacted laminates, which typically contain delaminations in nearly every interface [23]. Similar studies have compared the residual compression strength of virgin laminates, or laminates that had implanted delaminations in a single interface, to identical laminates without implants that had undergone low-velocity impact with subsequent cycling [24,25]. For example, Fig. 10 shows a plot of cycles to failure as a function of stress amplitude for [0/90/0/45/ -45/0]s graphite/epoxy laminates subjected to fully reversed cyclic loading, either in the initially undamaged state, or following an impact with a energy per unit thickness of 1790 J/m [25]. The data in Fig. 10 indicate that the compression strength after impact is very low compared with the fatigue behavior of the virgin laminate. Furthermore, most of the strength reduction occurs after the impact, with very little degradation due to subsequent cyclic loading.

For composites loaded in compression, final failure is not necessarily determined by the local strain concentration in the zero-degree plies, but often results from a global instability that occurs after delaminations accumulate through the thickness and become locally unstable. The sublaminates that are formed by the delaminations may buckle locally which in turn may lead to more delaminations forming in adjacent interfaces and subsequently buckling. Because of this progressive buckling mode of failure, compression fatigue lives are typically much lower than tension fatigue lives for identical laminates subjected to identical load amplitudes [25]. Combined tension/compression fatigue lives may be reduced even further as a result of delaminations forming from matrix cracks under tension loads and then growing as a result of local instabilities under the compression loads [26]. In each case, however, the final failure results from an accumulation of delaminations through the thickness. The damage-threshold/fail-safety approach could be used to estimate fatigue lives in each case. First, delamination onset would be predicted using an appropriate analysis for G depending upon the source of the original

850

delamination. Next, delaminations would be assumed to grow throughout the interface immediately, or solutions for instability driven delamination growth in compression would have to be incorporated if stiffness loss could not be monitored directly in real time. Several fracture mechanics models have been developed for the growth of through-width and elliptical patch delaminations in a single interface [27,28] These analyses would have to be extended to model laminates with multiple edge delaminations to simulate compression fatigue damage and laminates with multiple delaminations that were formed by matrix cracks to simulate tension/compression fatigue damage. Finally, fail safety may be assessed in compression, as delaminations form near the surface and then accumulate through the thickness, using appropriate analyses for local and global buckling of the damaged laminate.

These same models could be used to evaluate the consequence of low-velocity impact damage. Previous studies have shown that low-velocity impact damage develops as extensive matrix cracking and associated delaminations through the thickness [23,29]. Delamination onset in these cases has been modeled as delaminations initiating from matrix cracks under bending loads [30]. In brittle matrix composites, impacts that are barely visible on the impacted surface may be extensive throughout the laminate thickness. This extensive delamination results in greatly reduced compression strength. Subsequent cyclic loading may create only slightly greater damage growth, which would explain the relatively flat S-N curves observed for impacted brittle matrix laminates (Fig. 10). Tougher matrix composites, however, suppress some of the delaminations that would otherwise form through the thickness during the impact [29]. Therefore, the compression strength following impact is greater than the compression strength for similar laminates with brittle matrices, but cyclic loading subsequent to an impact may cause further damage and corresponding reductions in residual compression strength. In either case, the damage-threshold/fail-safety approach may be used to characterize the delamination onset and assess the fail safety of the damaged laminate.

PART II: CONTINUUM DAMAGE MODEL

The foundation of the progressive failure methodology developed by Allen and Harris is a constitutive relationship which analytically predicts damage-dependent laminate stiffness properties and damage-dependent ply level stresses. The kinematic effects of microstructural damage are introduced into the constitutive relationship by an internal state variable (ISV). The ISV's are strain-like quantities which are mathematically expressed as second-order tensors. Progressive damage development is accounted for by specifying the loading history dependent present value of the ISV's. The present value of any specific ISV is calculated from a damage growth law which depends on both the loading history and the present value of any other operative damage mechanism. The constitutive relationship and the ISV growth laws form the mechanics framework for a "damage model" which has the potential to predict sublaminate damage accumulation and laminate failure.

The primary objective of a progressive failure methodology is to predict the residual strength and life of structural components. Since these components may have many dif-

ferent geometries and laminate stacking sequences, it is essential that the required inputs to the damage model be independent of geometry and stacking sequence. In other words, the damage model must be capable of explicitly predicting the effects of geometry and stacking sequence on damage development and failure. Therefore, the approach taken to achieve this objective is to construct a nonlinear damage-dependent lamination theory (damage model) which can be implemented to any computational structural algorithm such as a finite element code. This then allows for modification of linear elastic codes via a time stepping scheme to account for load history dependent damage and an iterative algorithm to account for nonlinearity on each time step. The necessary parts of the damage model are as follows: 1) a kinematic description of the damage state (ISV's); 2) a damage dependent lamination theory which models the effects of interply delaminations; 3) a set of damage growth laws for predicting the load history dependence of the damage state at each material point; 4) a structural algorithm for modelling the response of components with spatially variable and load history dependent stresses and damage; and 5) residual strength and life prediction based on a failure function for unstable crack growth. Each of the above steps will be reviewed briefly in the following sections.

Kinematic Description of the Damage State

It is hypothesized that a local volume element may be selected which is small compared to the structural component of interest and, at least for the case of matrix cracking, the damage can be assumed to be homogeneous in this element. It is further hypothesized that the effects of the microcracks within this volume element may be locally averaged on a scale which is small compared to the structural component. A straightforward and direct approach to averaging the kinematic effects of cracks within the local volume element was taken by Vakulenko and M. L. Kachanov in 1971 [31]. This average is given by the following second order tensor:

$$\alpha_{ij}^{M} = \frac{1}{V_L} \int_{S_c} u_i^c n_j^c dS \tag{3}$$

where α_{ij}^{M} is the internal state variable (ISV) for the microcracking contained in the local volume (V_L), u_i^c are crack opening displacements in V_L, n_j^c are the components of a unit normal to the crack faces, and S_c is the surface area of matrix cracks in V_L, as shown in Fig. 11. It is significant to note that the deformed geometry shown in Fig. 11 gives rise to a physical interpretation of the ISV. Consider the perceived macroscale strain to be defined by the relative positions of points A"0'B" which consist of the material deformation state A"0"B" plus the relative crack face displacement 0'0". Then the ISV defined by equation (3) is the value of the crack face displacements integrated over the crack surface area and divided by an appropriately defined local volume. The ISV is, therefore, a strain-like quantity representing the average kinematic effects of the microcrack within a local volume of material.

Since matrix cracks are contained within an individual ply, or a grouping of adjacent plies with the same fiber orientation, the local volume for matrix cracks may be defined at the ply level. Ply level stress-strain equations may then be defined by integrat-

852

ing the governing field equations over a homogeneous local volume within which the effects of matrix cracks are introduced as a strain-like quantity by the ISV given in equation (3). The complete mathematical formulation is given in Reference 32.

The definition of the ISV given by equation 3 has a physical interpretation. Therefore, micromechanics and fracture mechanics approaches may be used to develop ISV mathematical models for specific cracks. However, this approach is quite cumbersome. A phenomenological approach is more straightforward provided a testing procedure can be defined which isolates the individual modes of cracking. In this approach, stiffness loss is experimentally determined as a function of the damage state and the ISV's are specified from the resulting empirical relationship. The authors have extensively employed this latter technique to specify the ISV's for matrix crack damage [33]. The appropriateness of this approach was verified for the case of matrix cracks in the 90° plies of cross-ply laminates by comparing the empirical results to those determined rigorously by using equation (3) and a micromechanics analysis to determine the crack-opening displacements [34].

Damage Dependent Lamination Theory

Unlike the ply level model for matrix cracking, spatial homogeneity cannot be assumed for delaminations. Even if the delaminations may appear to be evenly distributed in the plane of the laminate, the same cannot be said for the through-thickness direction. The damage is, therefore, accounted for by area averaging in the laminate plane, accompanied by a kinematic assumption through the thickness. Accordingly, the laminate equations are constructed by assuming that the Kirchhoff-Love hypothesis may be modified to include the effects of jump displacements u_i^D, v_i^D, and w_i^D as well as jump rotations β_i^D and ψ_i^D for the ith delaminated ply interface, as shown in Fig. 12. The displacement fields in the x, y, and z directions are mathematically defined as

$$u(x,y,z) = u^o(x,y) - z\left[\beta^o + H(z - z_i)\beta_i^D\right] + H(z - z_i)u_i^D \qquad (4)$$

$$v(x,y,z) = v^o(x,y) - z\left[\psi^o + H(z - z_i)\psi_i^D\right] + H(z - z_i)v_i^D \qquad (5)$$

and

$$w(x,y,z) = w^o(x,y) + H(z - z_i)w_i^D \qquad (6)$$

where the superscripts "o" imply undamaged midsurface quantities, and $H(z-z_i)$ is the Heavyside step function. Also, a repeated index i in a product is intended to imply summation, and the supercripts D imply displacement components across the delamination. Locally averaging the above equations and applying standard lamination theory will result in the following laminate equations [32]:

$$\{N\} = \sum_{k=1}^{n} [Q]_k (z_k - z_{k-1})\{\varepsilon_L^0\} - \tfrac{1}{2}\sum_{k=1}^{n}[Q]_k (z_k^2 - z_{k-1}^2)\{\kappa_L\} + \tag{7}$$

$$\sum_{l=1}^{d} [\overline{Q_1}]_l\, t_l \begin{Bmatrix} 0 \\ \alpha_{1l}^D \\ \alpha_{2l}^D \\ \alpha_{3l}^D \\ 0 \end{Bmatrix} + \sum_{l=1}^{d}(z_l - z_{l-1})[\overline{Q_2}]_l \begin{Bmatrix} 0 \\ 0 \\ \alpha_{4l}^D \\ \alpha_{5l}^D \\ 0 \end{Bmatrix} - \sum_{k=1}^{n}(z_k - z_{k-1})[Q]_k\{\alpha^M\}_k$$

$$\{M\} = \tfrac{1}{2}\sum_{k=1}^{n} [Q]_k (z_k^2 - z_{k-1}^2)\{\varepsilon_L^0\} - \tfrac{1}{3}\sum_{k=1}^{n}[Q]_k (z_k^3 - z_{k-1}^3)\{\kappa_L\} + \tag{8}$$

$$\sum_{l=1}^{d} [\overline{Q_3}]_l\, t_l^2 \begin{Bmatrix} 0 \\ \alpha_{1l}^D \\ \alpha_{2l}^D \\ \alpha_{3l}^D \\ 0 \end{Bmatrix} + \sum_{l=1}^{d+1}(z_l^2 - z_{l-1}^2)[\overline{Q_4}]_l \begin{Bmatrix} 0 \\ 0 \\ \alpha_{4l}^D \\ \alpha_{5l}^D \\ 0 \end{Bmatrix} - \tfrac{1}{2}\sum_{k=1}^{n}[Q]_k(z_k^2 - z_{k-1}^2)\{\alpha^M\}_k$$

where {N} and {M} are the resultant forces and moments per unit length, respectively, and $\{\alpha^M\}_k$ and α_i^D represent the damage due to matrix cracking and interply delamination, respectively. Furthermore, n is the number of plies, and d is the number of delaminated ply interfaces. The ISV for delamination, α_i^D, has the same mathematical form as does equation (3) for general microcracking. All other terms in equations 7 and 8 have the standard lamination theory definitions.

An initial inspection of equations 7 and 8 raises the question of how many additional material constants and ISV's are required to include damage in the laminate equations. No additional material constants are required because the constants in $\overline{Q}_1$, $\overline{Q}_2$, $\overline{Q}_3$, and $\overline{Q}_4$ are related to the individual ply moduli as is Q. Unique ISV's are required for each ply developing matrix cracks and for each delamination. There are 3 unique ISV's for matrix cracks and 5 unique ISV's for delaminations. However, only 2 matrix crack ISV's and 1 delamination ISV are operative for symmetric laminates subjected to in-plane loading conditions. For the predictions reported in this paper, the matrix crack ISV's

are determined phenomenologically from test data obtained from $[0/90/0]_T$ and $[\pm 45]_{2S}$ laminates. The delamination ISV is determined analytically from strain energy release rate considerations. The mathematical expressions for the ISV's contain explicit laminate stacking sequence terms so that they may be used to model damage in any general laminate. The detailed development of these mathematical descriptions are given in reference 33.

A measure of the accuracy of laminate equations (7) and (8) can be obtained by comparing predictions of damage-dependent stiffness to experimental results. Predictions have been made for a typical graphite/epoxy system, AS4/3501-6. The bar chart shown in Fig. 13 compares the model predictions to the experimental values for the engineering modulus, E_x, for combined matrix cracking and delamination. The delamination interface location and percent of delamination area are listed in the figure underneath the laminate stacking sequence. As can be seen, the comparison between model results and the experimental results is quite good. Some limited results for Poisson's ratio are given in Fig. 14 using the same bar chart format.

A computer code has been constructed to determine the effect of damage on the average ply stresses in laminates [33]. Several laminates have been analyzed for an applied strain of $\varepsilon_{xo} = 0.01$ with all other components of strain being zero. Damage variables were calculated for the damage state determined experimentally using edge replication and x-ray radiography. The 90° plies use the matrix crack ISV α_{22}^M for normal extension while the off-axis plies use ISV α_{12}^M for shear deformation as well as α_{22}^M. No damage is assumed in the 0° plies. Since the laminate is subjected only to ε_{xo}, ISV α_{13}^D for shear deformation is assumed to be the only delamination damage component. The stress analysis results are shown in Table 1. Matrix cracks caused substantial stress reductions in ply stresses in the 90° plies in cross-ply laminates. For example, in the 90° plies of the $(0_2/90_2)_s$ laminate the matrix cracks resulted in a thirty-four percent average ply stress reduction. The two quasi-isotropic laminates developed different damage resulting in dissimilar far-field ply stresses. The $(90/\pm 45/0)_s$ laminate exhibited little matrix cracking, thus producing only a small reduction in ply stress in both the 90° and $\pm 45°$ plies. The $(0/\pm 45/90)_s$ laminate exhibited a similar stress reduction in the $\pm 45°$ plies, but showed a substantial stress reduction (fifteen percent verses one percent) in the 90° plies when compared to the $(90/\pm 45/0)_s$ laminate. This alteration in ply stresses should significantly affect the growth of new damage in the composite.

Damage Growth Laws

It is hypothesized that the growth of damage in each ply is driven by the current stress state at the crack tips within that ply [35]. The form of the damage growth law for matrix cracks currently implemented in the damage model is based on the observation made by Wang, et al. [36] that for some materials the damage growth rate per load step follows a power law with the strain energy release rate, G, and a material parameter, n, serving as the basis and exponent, respectively. To develop ISV growth law equations,

α_{ij}^M must be related to the surface area of damage and the far-field applied loads. To date, phenomenological growth laws have been developed only for matrix crack growth.

The growth law has been used to predict the matrix crack growth histories for two crossply laminates [37]. The model predictions for the damage state in $[0_2/90_2]_s$ laminates loaded in fatigue at R = 0.1 and maximum applied laminate stress of 38 ksi and 43 ksi are shown in Figs. 15 and 16, respectively. The lower stress is equivalent to eighty percent of the monotonic matrix crack initiation stress, while the higher stress is equal to ninety percent of the initiation stress. The experimentally measured damage states were originally specified in terms of the crack density. The corresponding ISV for each damage level can be approximated by the relationship proposed by Lee, et al. [34]. The damage growth for the thicker $[0_2/90_3]_s$ laminate is shown in Fig. 17. This laminate was loaded at a maximum laminate stress of 26 ksi. This stress corresponds to eighty percent of the monotonic matrix crack initiation stress. The results for this load case indicated good agreement with the experimental data. The effect of the load redistribution on the damage evolution is apparent in this load case. A decrease in the rate of damage growth after fifty thousand load cycles was predicted by the model. On the other hand, the experimental data showed this decrease to occur after only ten thousand load cycles. This decrease in the predicted rate of damage growth is attributed only to the matrix crack induced transfer of load from the 90° plies to the adjacent 0° plies and the resulting decrease in the available crack driving force. However, the experimental values of the damage growth rate may have been influenced by the formation of delaminations observed to occur along the free edges and in the interior.

To examine the amount of stress redistribution that occurs during the damage accumulation, the model was used to determine the axial stress in the 90° plies of the $[0_2/90_3]_s$ laminate loaded in fatigue at R = 0.1 and at three different maximum stresses. Fig. 18 shows that for the laminate stress of 38 ksi, the axial stress in the 90° plies after forty thousand cycles was less than fifty percent of the original stress level in the undamaged laminate. Therefore, the rate of damage growth is expected to be relatively low during the latter stages of the loading history because of the reduction in the ply-level stress. This is observed in Fig. 19, which shows the corresponding values of the ISV,

α_{22}^M , for the three load cases. The 26 ksi stress amplitude load case, on the other hand, produced only gradual changes in the axial stress and damage state as compared to the other two stress amplitudes. The percentage decrease from the original undamage stress level increased with the fatigue stress amplitude. These results demonstrate that the stress redistribution characteristics among the plies in the laminate are dependent on the loading conditions. These redistribution characteristics will affect the manner in which damage develops in the surrounding plies as well as the eventual failure of the laminate.

An Algorithm for Structural Analysis

In order to predict the response of a structural component with spatially variable stresses, it is necessary to incorporate the damage dependent lamination theory into a structural analysis algorithm. This was accomplished via the finite element method. A plate element formulation was achieved by integrating the governing plate equilibrium

856

equations against variations in the displacement components and employing Green's Theorem. The resulting formulation of the laminated plate equilibrium equations is described in detail in reference 38. These equations are then discretized spatially by the finite element method, which utilizes five degrees of freedom at each node. These consist of two in-plane displacements, one out-of-plane displacement, and two rotational terms.

A finite element code has been developed based on the above formulation and implemented for matrix crack growth. The implementation of the damage growth law requires that the solution algorithm be repeated for every load cycle. During each cycle, the ply stresses are calculated and used to determine the increment in the matrix crack ISV for each ply. The updated damage state is then used in the calculation of the laminate and ply response at the next load cycle.

The response of a laminated tapered plate subjected to an in-plane uniaxial fatigue loading condition has been examined. This beam has a $[0/90_2]_s$ stacking sequence and possesses the material properties of AS4/3501 graphite/epoxy. The plate length is 17.78 cm and the width is 4.50 cm at the clamped end and tapered to 2.87 cm at the end where the load is applied. The plate is loaded at a distributed load amplitude of 17.5×10^3 N/m and $R = 0.1$. Since the plate is symmetric about its length, it is sufficient to model half of the plate with a mesh containing 28 elements, 24 nodes, and 120 degrees of freedom. The spatial variation and growth of the matrix crack ISV's during the loading history in the 90° and 0° plies, is shown in Figs. 20 and 21, respectively. For clarity, the plotted values of the ISV's in each ply are normalized by the largest value of the ISV within that ply at the end of the loading history, 22500 cycles. The predicted results indicate that the matrix cracks first occur in the 90° plies at the narrow end and progress toward the wider end as loading continues. Axial splits in the 0° plies do not develop until after the appearance of the matrix cracks in the 90° plies. Thus, the matrix cracks accumulate in the 90° plies and load is transferred to the 0° plies. Depending on the amplitude of the fatigue load, more than half of the load initially carried by the undamaged 90° plies will be transferred to the 0° plies. The additional load carried by the 0° plies coupled with the stress concentrations caused by the matrix cracks in the 90° plies create suitable conditions for the growth of matrix cracks in the 0° plies. The results also show that the progression of matrix cracks along the length of the tapered beam decelerates near the midway point. The stresses in the region beyond the midway point are insufficient to promote additional damage growth. The matrix crack growth will increase at the narrow end until the matrix cracks have either reached the saturation level or the laminate fails.

Residual Strength and Life Prediction

Typically fiber fracture is the final damage event to occur in a laminate. Fiber fracture in the principal load-carrying plies may lead directly to catastrophic laminate failure. In this case, an ISV representing fiber fracture is not required and the fracture can be predicted by a ply level failure function such as the Tsai-Wu criterion [39]. However, stable fiber fracture may accumulate throughout a loading history. For example, fiber fracture may occur in the damage zone produced by a high strain gradient field at a geometric discontinuity such as an open hole or a bolt hole. In this case, significant load redistribution around the damage zone will occur prior to a catastrophic failure. An ISV

representing the kinematic effects of the fiber fracture will be necessary to accurately predict the local laminate stiffness and associated load redistribution. A global-local iterative analysis methodology will be necessary to distinguish between these two conditions. The logic flow of the global-local iterative analysis methodology required to predict laminate residual strength and life is shown in Fig. 22. Obviously a finite element based structural analysis would be required to facilitate this methodology.

Damage growth laws for delamination and fiber fracture are currently being developed and, once available, the damage model will be fully developed for tensile failure dominated structures. Following completion of these activities, the mechanics framework will be developed for compression failure. Once the compression failure mechanics are incorporated into the damage model, the methodology will be extended to treat impact damage. This formulation seems particularly well suited to predicting damage development during the impact event and subsequent damage growth. This is because the damage model will be incorporated into a finite element formulation which can be used to predict the structural dynamics characteristics of the impact event.

SUMMARY

The damage threshold/fail safety methodology developed by O'Brien assumes the existence of matrix cracks throughout the off-axis plies of the laminate and predicts delamination onset using a strain energy release rate characterization. Delamination growth is accounted for in one of three ways: either analytically, using delamination growth laws in conjunction with strain energy release rate analyses; experimentally, using measured stiffness loss; or conservatively, assuming delamination onset corresponds to catastrophic growth. Fail safety is assessed by accounting for the accumulation of delaminations through the laminate thickness. The utility of this approach has been demonstrated for predicting the tension fatigue life of graphite/epoxy, glass/ epoxy and hybrid laminates. In addition, this methodology can probably be employed to predict compression fatigue life and post impact residual strength.

The progressive failure methodology developed by Allen and Harris employs damage-dependent constitutive relationships to calculate damage-dependent ply level stresses which are then input into appropriate criteria to predict laminate failure. Using the concept of continuum damage mechanics, internal state variables (ISV's), defined for each mode of damage, are used to introduce the kinematic effects of damage into the laminate constitutive relationships. A global/local analysis strategy is used to calculate the global structural response to the applied loads and the local analysis is used to calculate the ply level stresses in high strain gradient fields produced by structural discontinuities such as circular cutouts. Damage growth laws for the ISV's are loading history dependent and, through an iterative process between the global/local analyses, are continuously updated until laminate failure is predicted. This methodology is in the process of being implemented into a finite element code for predicting the residual strength and life of structures under tensile loading but has not been developed, to date, for compressively loaded structure. Once compression failure is implemented, the methodology can be used in conjunction with a structural dynamics analysis to predict the formation of damage during an impact event.

858

Finally, the question of which methodology is preferred must be addressed. This, of course, is problematic because one method may be preferred for some applications and the second method for other applications. The damage tolerance/fail safety method is well suited for initial design analyses while the "automated" features of the continuum damage model are well suited for detailed finite element stress analyses. If it is not practical to model sublaminate damage as free surfaces, the continuum damage model also offers the versatility of describing the effects of damage on load redistribution at the global structural level. However, the continuum damage mechanics approach must be coupled with a local analysis such as fracture mechanics or the damage tolerance/fail safety method to predict material level sublaminate damage growth and subsequent failure.

REFERENCES

[1] Wilkins, D. J.; Eisenmann, J. R.; Camin, R. A.; Margolis, W. S.; and Benson, R. A.: Characterizing Delamination Growth in Graphite-Epoxy, Damage in Composite Materials, ASTM STP 775, American Society for Testing and Materials, June 1982, p. 168.

[2] Mall, S.; Yun, K. T.; and Kochnar, N. K.: Characterization of Matrix Toughness Effects on Cyclic Delamination Growth in Graphite Fiber Composites. ASTM STP 1012, April 1989, pp. 296-312.

[3] Russell, A. J. and Street, K. N.: Predicting Interlaminar Fatigue Crack Growth Rates in Compressively Loaded Laminates, ASTM STP 1012, April 1989 pp. 162-180.

[4] Gustafson, C. G. and Hojo, M.: Delamination Fatigue Crack Growth in Unidirectional Graphite/Epoxy Laminates, Journal of Reinforced Plastics, Vol. 6, No. 1, January 1987, pp. 36-52.

[5] O'Brien, T. K.: Generic Aspects of Delamination in Fatigue of Composite Materials, Journal of the American Helicopter Society, Vol. 32, No. 1, January 1987, pp. 13-18.

[6] Martin, R. H. and Murri, G. B.: Characterization of Mode I and Mode II Delamination Growth and Thresholds in Graphite/PEEK Composites, ASTM STP 1059, pp. 251-270.

[7] O'Brien, T. K.: Characterization of Delamination Onset and Growth in a Composite Laminate, Damage in Composite Materials, ASTM STP 755, American Society for Testing and Materials, 1982, pp. 140-167.

[8] Russell, A. J. and Street, K. N.: Moisture and Temperature Effects on the Mixed-Mode Delamination Fracture of Unidirectional Graphite/Epoxy, Delamination and Debonding of Materials, ASTM STP 876, American Society for Testing and Materials, October 1985, pp. 349-370.

9] Poursartip, A.: The Characterization of Edge Delamination Growth in Composite Laminates Under Fatigue Loading, Toughened Composites, ASTM STP 937, American Society for Testing and Materials, 1987, pp. 222-241.

[10] O'Brien, T. K.: Mixed-Mode Strain Energy Release Rate Effects on Edge Delamination of Composites, Effects of Defects in Composite Materials, ASTM STP 836, American Society for Testing and Materials, 1984, pp. 125-142.

[11] O'Brien, T. K.: Tension Fatigue Behavior of Quasi-Isotropic Graphite/Epoxy Laminates, Fatigue and Creep of Composite Materials, Proceedings, 3rd Riso International Symposium on Metallurgy and Materials Science, Riso National Laboratory, Roskilde, Denmark, 1982, pp. 259-264.

[12] O'Brien, T. K.: Fatigue Delamination Behavior of PEEK Thermoplastic Composite Lamines, Journal of Reinforced Plastics, Vol. 7, No. 4, July 1988, pp. 341-359.

[13] O'Brien, T. K.; Murri, G. B.; and Salpekar, S. A.: Interlaminar Shear Fracture Toughness and Fatigue Thresholds for Composite Materials, Composite Materials: Fatigue and Fracture--Second Volume, ASTM STP 1012, American Society for Testing and Materials, 1989, pp. 222-250.

[14] Adams, D. F.; Zimmerman, R. S.; and Odem, E. M.: Frequency and Load Ratio Effects on Critical Strain Energy Release Rate G_c Thresholds of Graphite Epoxy Composites, Toughened Composites, ASTM STP 937, American Society for Testing and Materials, Philadelphia, 1987, p. 242.

[15] O'Brien, T. K.; Rigamonti, M.; and Zanotti, C.: Tension Fatigue Analysis and Life Prediction for Composite Laminates, International Journal of Fatigue, Vol. 11, No. 6, Nov. 1989, pp. 379-394.

[16] O'Brien, T. K.: Analysis of Local Delaminations and Their Influence on Composite Laminate Behavior, Delamination and Debonding of Materials, ASTM STP 876, American Society for Testing and Materials, 1985, pp. 282-297.

[17] Caslini, M.; Zanotti, C.; and O'Brien, T. K.: Study of Matrix Cracking and Delamination in Glass/Epoxy Laminates, Journal of Composites Technology and Research, Vol. 9, No. 4, Winter 1987, pp. 121-130.

[18] O'Brien, T. K.; Crossman, F. W.; and Ryder, J. R.: Stiffness, Strength, and Fatigue Life Relationships for Composite Laminates, Proceedings, Seventh Annual Mechanics of Composites Review, AFWAL-TR-82-4007, Air Force Wright Aeronautical Laboratories, Dayton, OH, April 1982, pp. 79-90.

[19] O'Brien, T. K.: The Effect of Delamination on the Tensile Strength of Unnotched, Quasi-Isotropic, Graphite Epoxy Laminates, Proceedings, SESA/JSME Joint Conference on Experimental Mechanics, Honolulu, HI, May 1982, Part I, SESA, Brookfield Center, CT, pp. 236-243.

[20] Ryder, J. T. and Crossman, F. W.: A Study of Stiffness, Residual Strength, and Fatigue Life Relationships for Composite Laminates, NASA CR-172211, National Aeronautics and Space Administration, Washington, DC, October 1983.

[21] Jamison, R. D.; Schulte, K.; Reifsnider, K. L.; and Stinchcomb, W. W.: Characterization and Analysis of Damage Mechanisms in Tension-Tension Fatigue of Graphite/Epoxy Lamines, Effects of Defects in Composite Materials, ASTM STP 836, American Society for Testing and Materials, 1984, pp. 21-55.

[22] McCarty, J. E. and Ratwani, M. M.: Damage Tolerance of Composites, Interim Report No. 3, AFWAL Contract F33615-82-C-3213, Boeing Military Airplane Co., Dayton, OH, March 1984.

[23] Guynn, E. G. and O'Brien, T. K.: The Influence of Lay-up and Thickness on Composite Impact Damage and Compression Strength, AIAA-85-0646, Proceedings, 26th AIAA/ASME/ASCE/AHS Structures, Structural Dynamics, and Materials Conference, Orlando, FL, April 1985, pp. 187-196.

[24] Byers, D. A.: Behavior of Damaged Graphite/Epoxy Laminates Under Compression Loading, NASA CR 159293, National Aeronautics and Space Administration, Washington, DC, August 1980.

[25] Bishop, S. M. and Dorey, G.: The Effect of Damage on the Tensile and Compressive Performance of Carbon Fiber Laminates, Characterization, Analysis, and Significance of Defects in Composite Materials, AGARD CP-355, Advisory Group for Aerospace Research and Development, Paris, April 1983.

[26] Bakis, C. E. and Stinchcomb, W. W.: Response of Thick, Notched Laminates Subjected to Tension-Compression Cyclic Loads, Composite Materials: Fatigue and Fracture, ASTM STP 907, American Society for Testing and Materials, Philadelphia, June 1986, pp. 314-334.

[27] Chai, H.; Babcock, D. D.; and Knauss, W. G.: One-Dimensional Modeling of Failure in Laminated Plates by Delamination Buckling, International Journal of Solids and Structures, Vol. 17, No. 11, pp. 1069-1083.

[28] Whitcomb, J. D.: Finite Element Analysis of Instability-related Delamination Growth, Journal of Composite Materials, Vol. 15, 1981, pp. 403-426.

[29] Carlile, D. R. and Leach, D. C.: Damage and Notch Sensitivity of Graphite/PEEK Composite, Proceedings, 15th National SAMPE Technical Conference, October 1983, pp. 82-93.

[30] Murri, G. B. and Guynn, E. G.: Analysis of Delamination Growth from Matrix Cracks in Laminates Subjected to Bending Loads, Composite Materials: Testing and Design, (Eighth Conference), ASTM STP 972, American Society for Testing and Materials, 1988, pp. 322-339.

[31] Vakulenko, A. A.and Kachanov, M. L.: Continuum Theory of Cracked Media, Izv. AN SSR, Mekhanika Tverdogo Tela, Vol. 6, p. 159, 1971.

[32] Allen, D. H.: Groves, S. G.;and Harris, D. C.: A Cumulative Damage Model for Continuous Fiber Composite Laminates with Matrix Cracking and Interply Delamination, Composite Materials: Testing and Design (8th Conference), ASTM STP, American Society for Testing and Materials, 1987.

[33] Allen, D. H.; Nottorf, E. W.; and Harris, C. E.: Effect of Microstructural Damage on Ply Stresses in Laminated Composites, Recent Advances in the Macro- and Micro-Mechanics of Composite Materials Structures, AD-Vol. 13, ASME, pp. 135-146, 1988.

[34] Lee, J. W.; Allen, D. H.; and Harris, C. E.: Internal State Variable Approach for Predicting Stiffness Reductions in Fibrous Laminated Composites With Matrix Cracks, Journal of Composite Materials, Vol. 23, pp. 1273-1291, 1989.

[35] Allen, D. H.; Harris, C. E.; and Groves, S. E.: A Thermomechanical Constitutive Theory for Elastic Composites with Distributed Damage - Part I: Theoretical Development, Int. Journal Solids & Structures, Vol. 23, No. 9, pp. 1301-1318, 1987.

[36] Wang, A. S. D.; Chou, P. C.; and Lei, S. C.: A Stochastic Model for the Growth of Matrix Cracks in Composite Laminates, Journal of Composite Materials, Vol. 18, pp. 239-254, 1984.

[37] Lo, D. C.; Allen, D. H.;and Harris, C. E.: A Continuum Model for Damage Evolution in Laminated Composites, Proceedings IUTAM Symposium, Troy, N.Y., 1990 (to appear).

[38] Buie, K. D.: A Finite Element Model for Laminated Composite Plates with Matrix Cracks and Delaminations, Texas A&M University Thesis, December, 1988.

[39] Tsai, S. W. and Wu, E. M.: A General Theory of Strength for Anisotropic Materials, Journal Composite Materials, pp. 58-80, 1971.

Table 1 PLY STRESSES RESULTING FROM MATRIX
CRACKING AND DELAMINATION

LAMINATE	PLY	INITIAL PLY STRESS σ (ksi)	STRESS W/MATRIX CRACKS σ (ksi)	STRESS W/MATRIX CRACKS & DELAM. σ (ksi)	DELAMINATION LOCATION MAGNITUDE (%) ISV α_{13}^D	MATRIX DAMAGE ISV's α_{22}^M	α_{12}^M
$[0/90]_s$	0	211.4	211.4	211.4	0/90	0	0
	90	14.0	9.6	8.5	16.6% .00076	.00318	0
$[0/90_2]_s$	0	211.4	211.4	211.4	0/90	0	0
	90	14.0	9.5	7.9	24.2%	.00326	0
	90	14.0	9.5	7.9	.001109	.00326	0
$[0_2/90_2]_s$	0	211.4	211.4	211.4		0	0
	0	211.4	211.4	211.4	0/90	0	0
	90	14.0	9.2	6.0	49.5%	.00344	0
	90	14.0	9.2	6.0	.002267	.00344	0
$[0/90_3]_s$	0	211.4	211.4	211.4		0	0
	90	14.0	10.6	8.3	0/90	.00247	0
	90	14.0	10.6	8.3	35.3%	.00247	0
	90	14.0	10.6	8.3	.001617	.00247	0
$[0/\pm45/90]_s$	0	211.4	211.4	211.4		0	0
	45	64.4	64.0	64.0	-45/90	0	.00067
	-45	64.4	64.0	64.0	57%	0	-.00067
	90	14.0	11.8	8.2	.002611	.00157	0
$[90/\pm45/0]_s$	90	14.0	13.9	13.9		.00060	0
	+45	64.4	64.0	64.0	+45/-45	0	.00067
	-45	64.4	64.0	48.7	52%	0	-.00067
	0	211.4	211.4	161.0	.002382	0	0
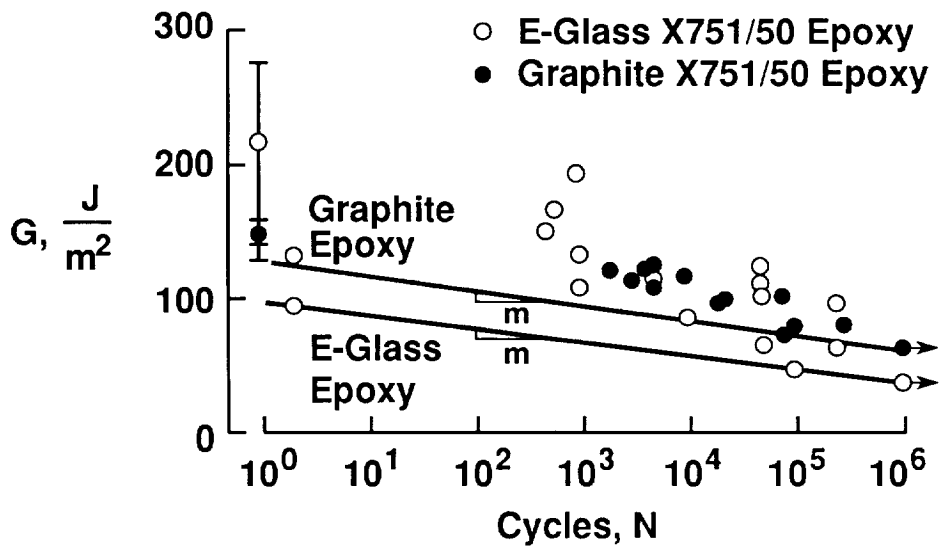
Figure 1. Comparison of Lower Bound Delamination Onset
Criteria for E-Glass Epoxy and Graphite Epoxy.

(a) Characterization of
delamination onset
and growth

(b) Prediction of delamin-
ation growth with
fatigue cycles

(c) Prediction of
stiffness loss with
fatigue cycles
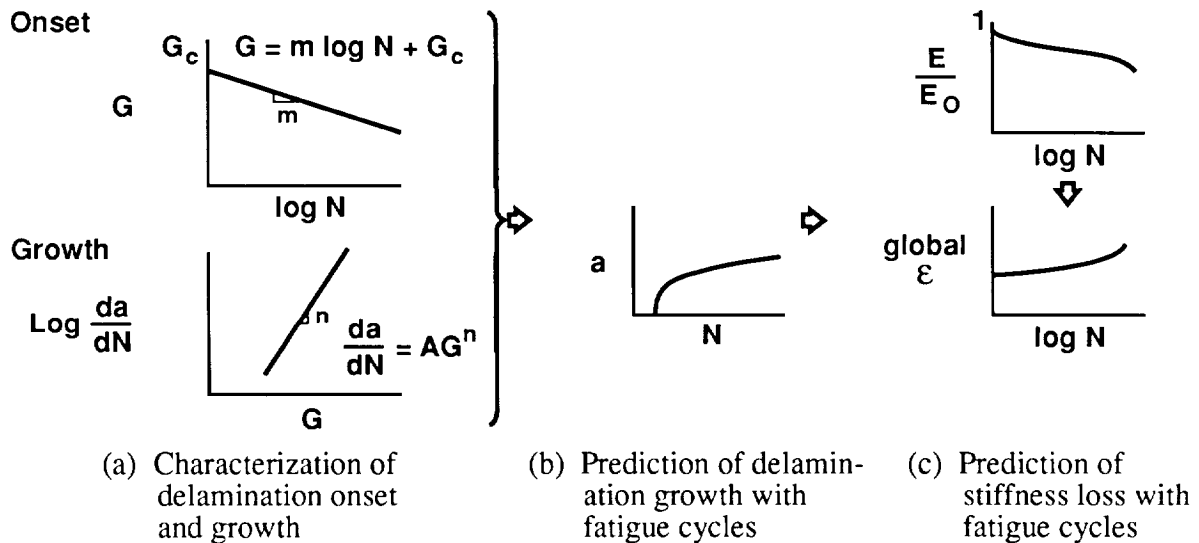
Figure 2. Prediction of stiffness loss due to delamination
in composite laminates.
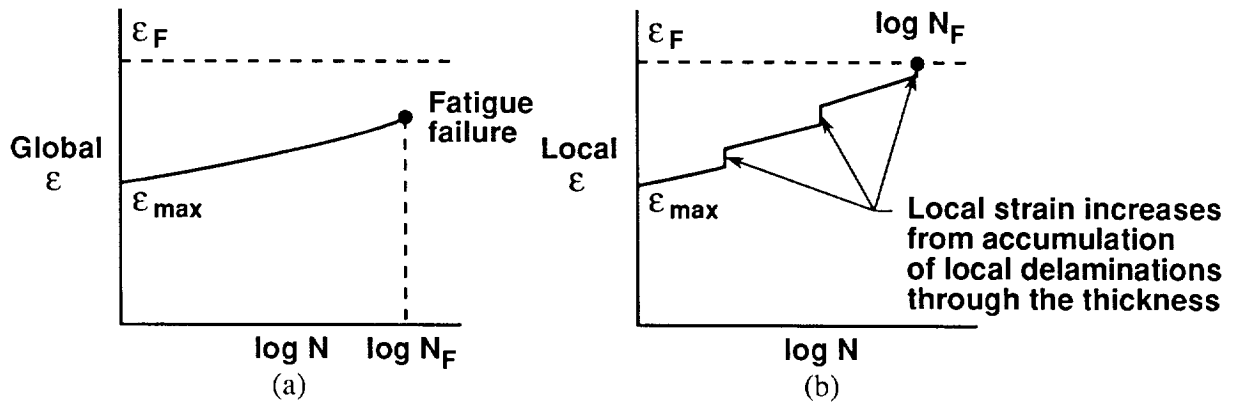
Figure 3. Increase in global versus local strain in 0° plies.

(a) Local $\varepsilon = K_\varepsilon \varepsilon_{MAX}$

(b) $(\varepsilon_F)_i = \dfrac{\varepsilon_F}{(K_\varepsilon)_i}$
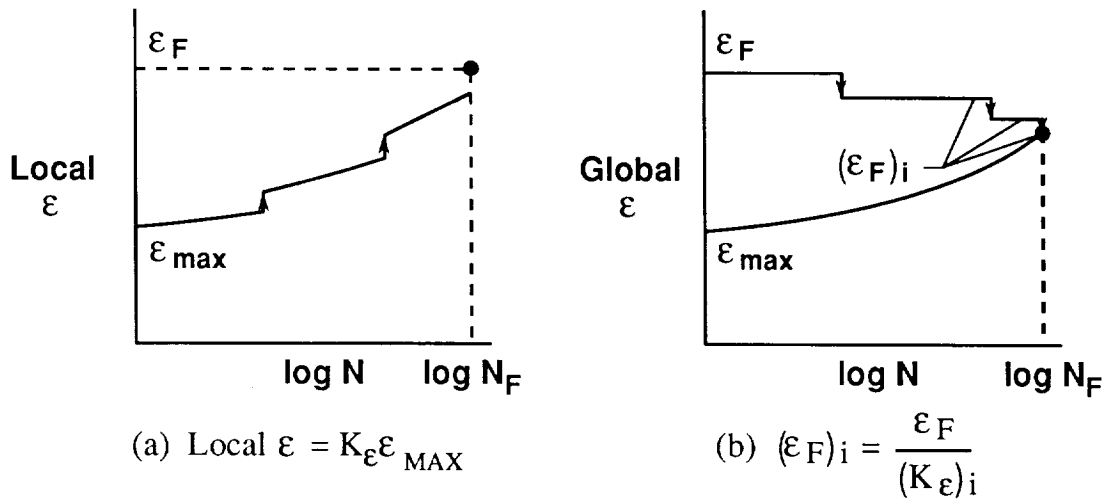
Figure 4. Effective reduction in ε_F due to local delamination accumulation through the laminate thickness.

$$t_{LAM}, E_{LAM}$$

$$G = \frac{\sigma^2 t_{LAM}^2}{2}\left(\frac{1}{E_{LD}t_{LD}} - \frac{1}{E_{LAM}t_{LAM}}\right)$$

$$t_{LD}, E_{LD} \longrightarrow t_{LAM}, E_{LAM}$$

Under constant σ_{max}, as local delaminations accumulate through-the-thickness, G changes for each case

$\therefore$ for the ith case

$$t_{LD}, E_{LD} \longrightarrow t_{LAM}, E_{LAM}$$

$$G_i(N) = m\log N_i + G_c = \frac{\sigma_{max}^2 t_{LAM}^2}{2}\left(\frac{1}{t_{LD}E_{LD}} - \frac{1}{t_{LAM}E_{LAM}}\right)_i$$

$$t_{LD}, E_{LD} \longrightarrow t_{LAM}, E_{LAM}$$

$$t_{LD}, E_{11}$$
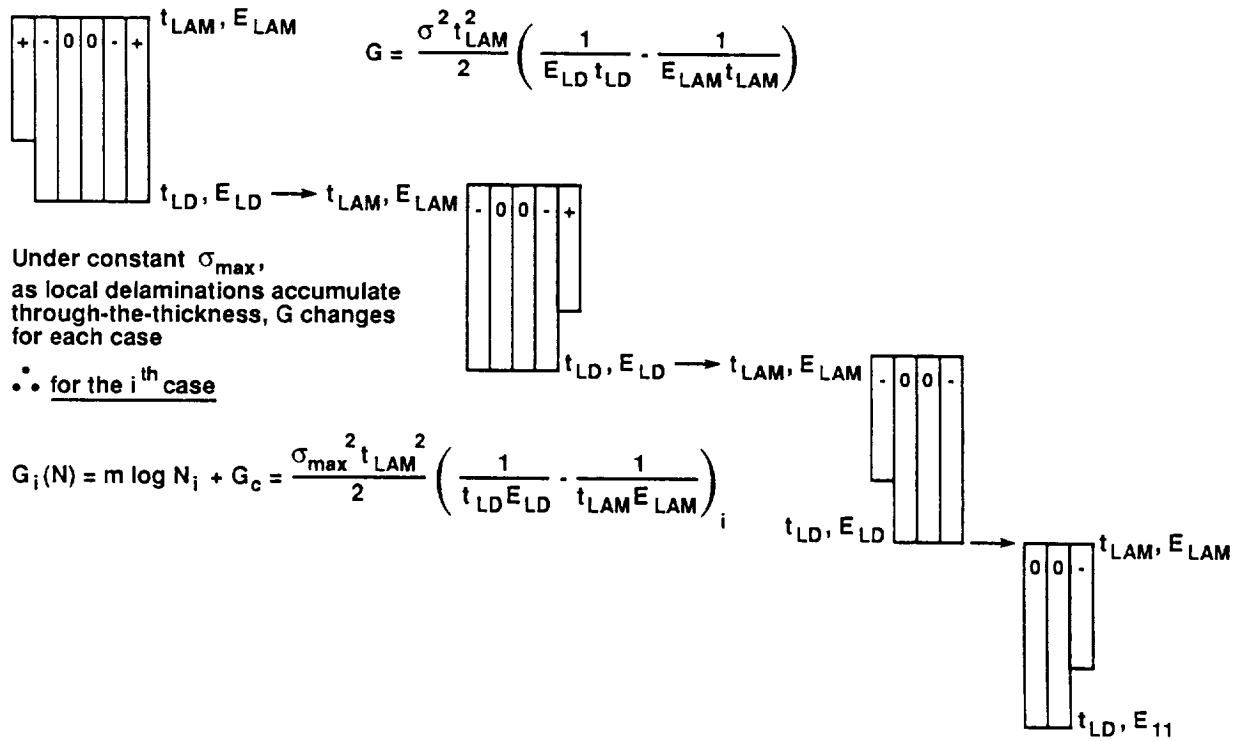
Figure 5. Strain energy release rate for local delamination onset.
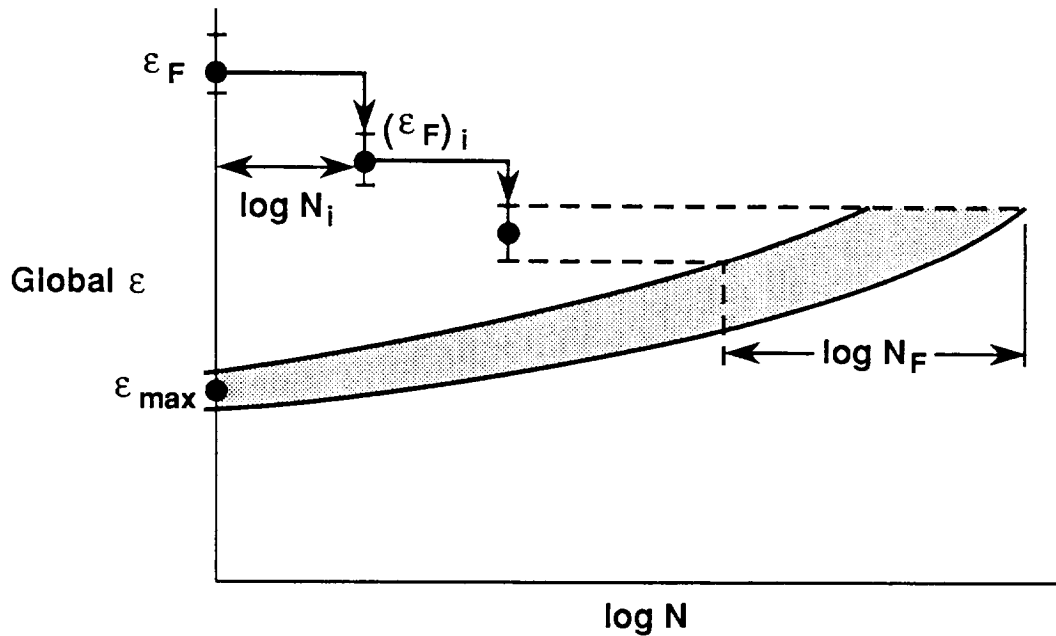
Figure 6. Tension fatigue life prediction for composite laminates. (σ_{max} = constant)
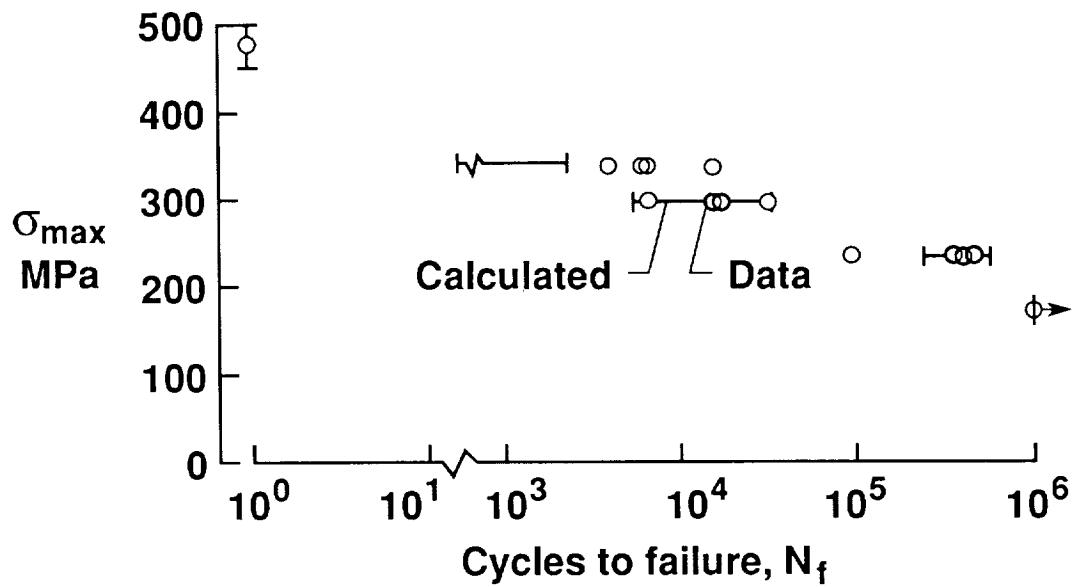
Figure 7. Fatigue Life Determination for $(45/-45/0)_s$ Graphite/E-Glass Epoxy Hybrid Laminates.
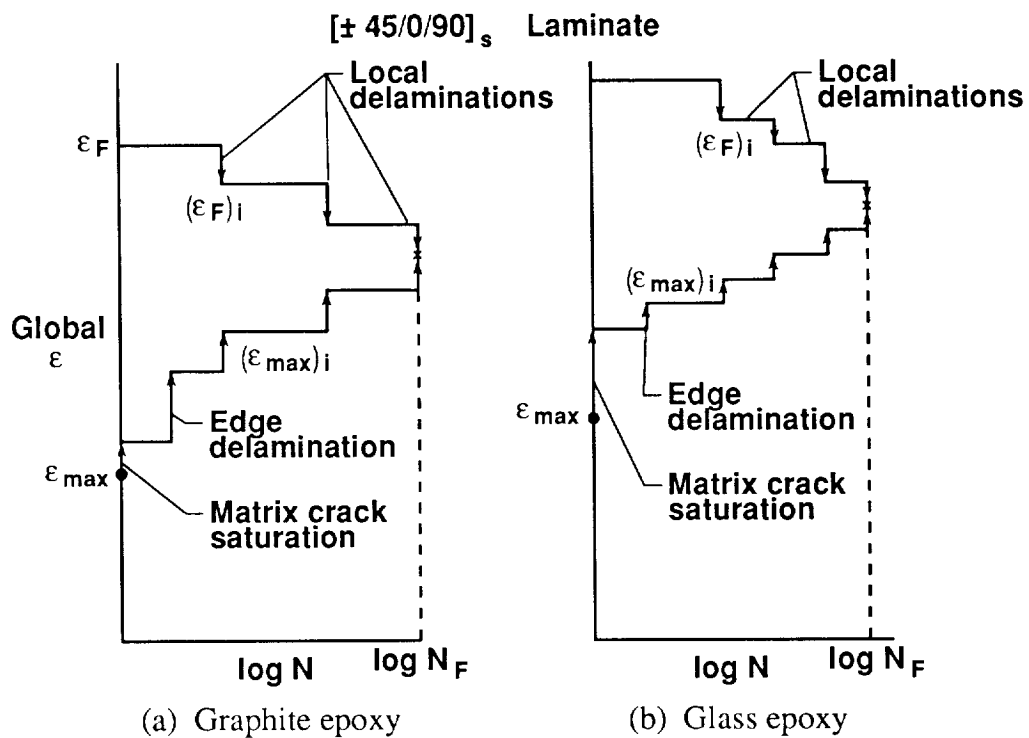
Figure 8. Damage-threshold/fail-safety analysis.
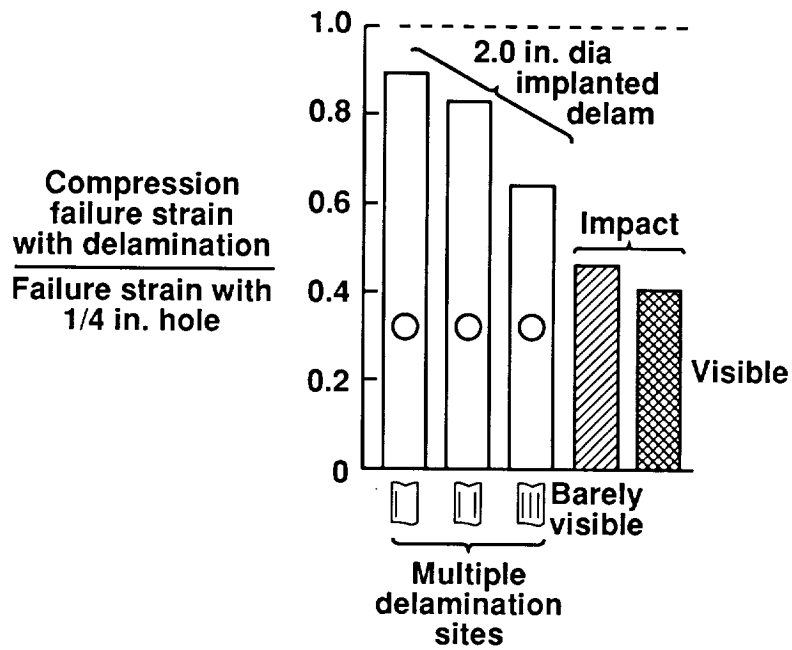
Figure 9. Normalized compression failure strain reduction
for laminates with implanted delaminations
or impact damage.
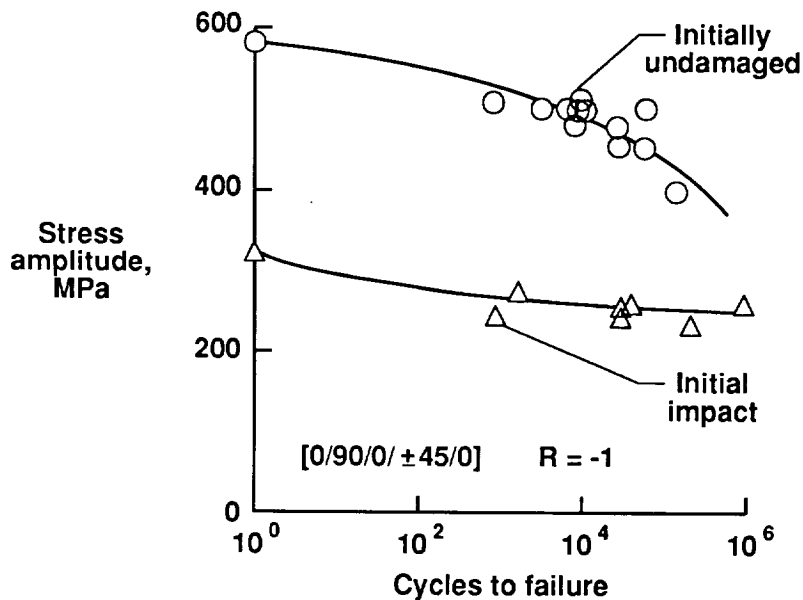
Figure 10. Fatigue behavior of initially undamaged and
impacted graphite/epoxy laminates under fully
reversed cyclic loading.
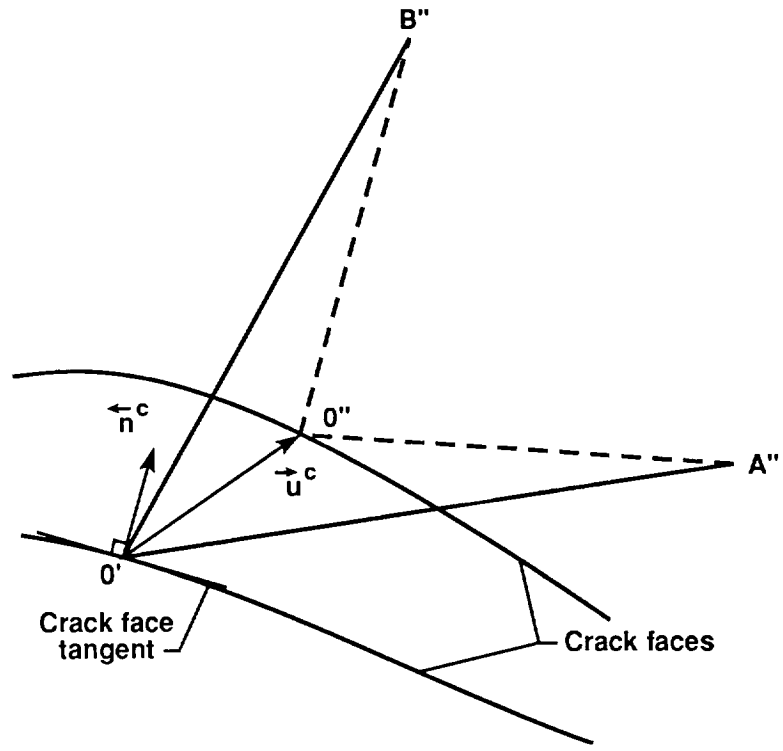
Figure 11. Local delamination and internal state variable
defined for material point 0'.
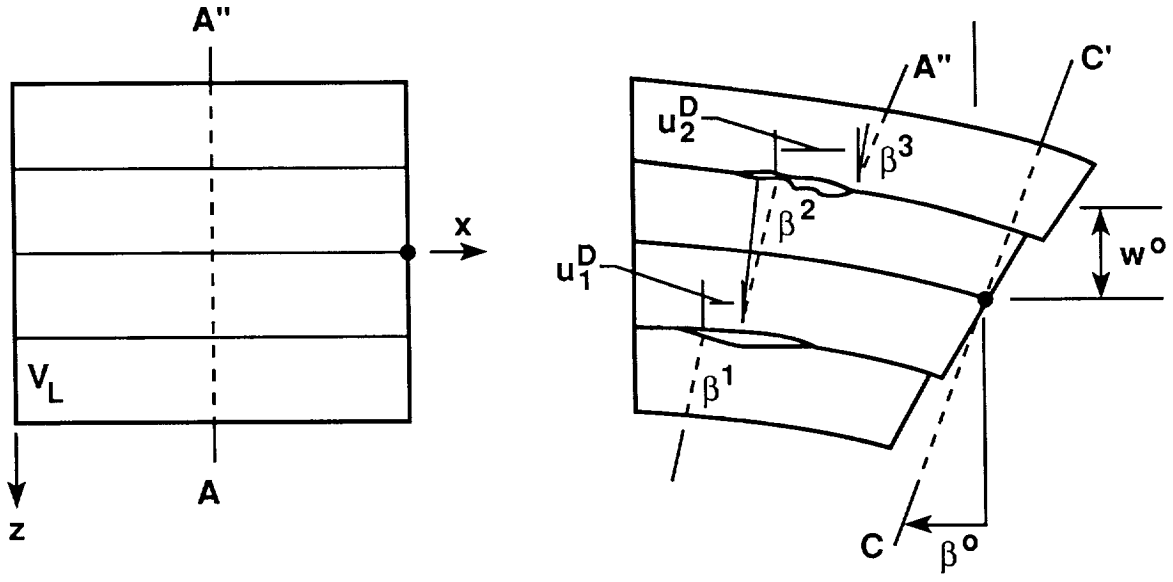
Figure 12. Discontinuities in the through-the-thickness
deformation due to delaminations.
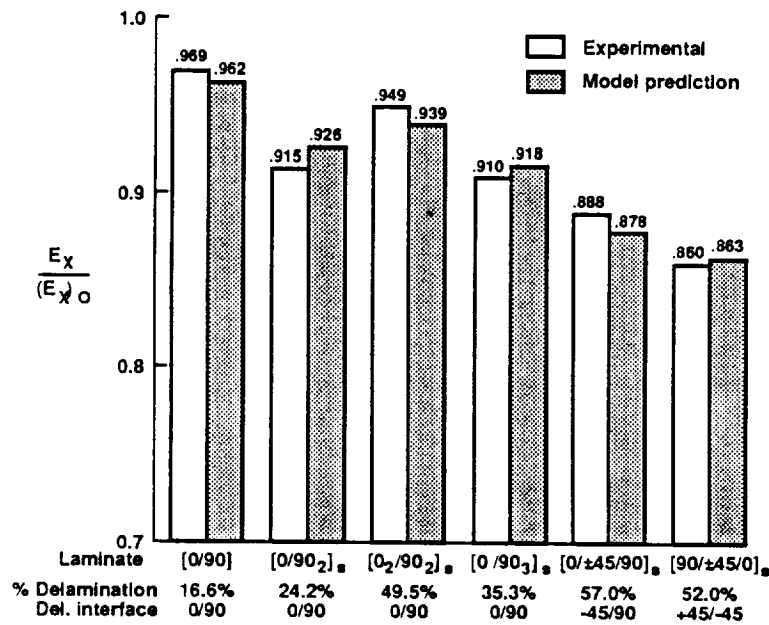
Figure 13. Comparison of experimental results and model predictions of the laminate engineering modulus, E_X, degraded by both matrix cracking and delamination damage.
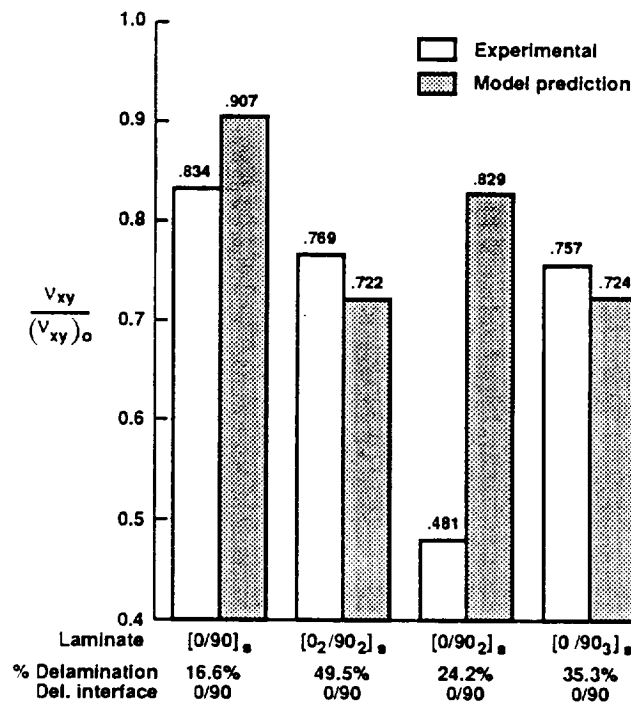
Figure 14. Comparison of experimental results and model predictions of the laminate engineering Poisson's ratio, v_{xy}, degraded by both matrix cracking and delamination damage.
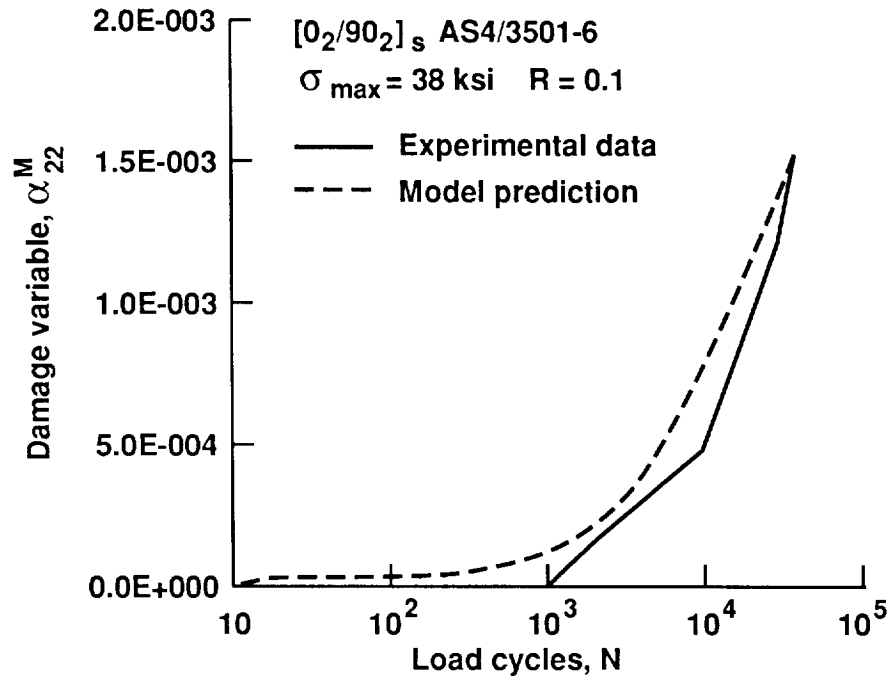
Figure 15. Matrix crack damage in the 90 plies of a $[0_2/90_2]_s$ laminate for a maximum applied laminate stress of 38 ksi and R = 0.1.
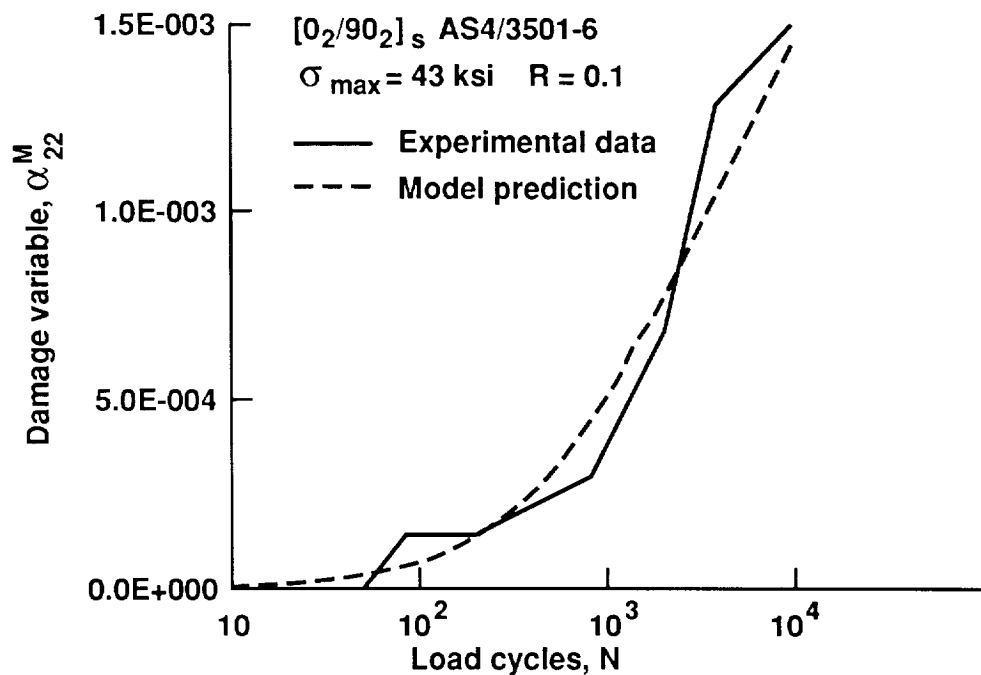

Figure 16. Matrix crack damage in the 90° plies of a $[0_2/90_2]_s$ laminate for a maximum applied laminate stress of 43 ksi and R = 0.1.
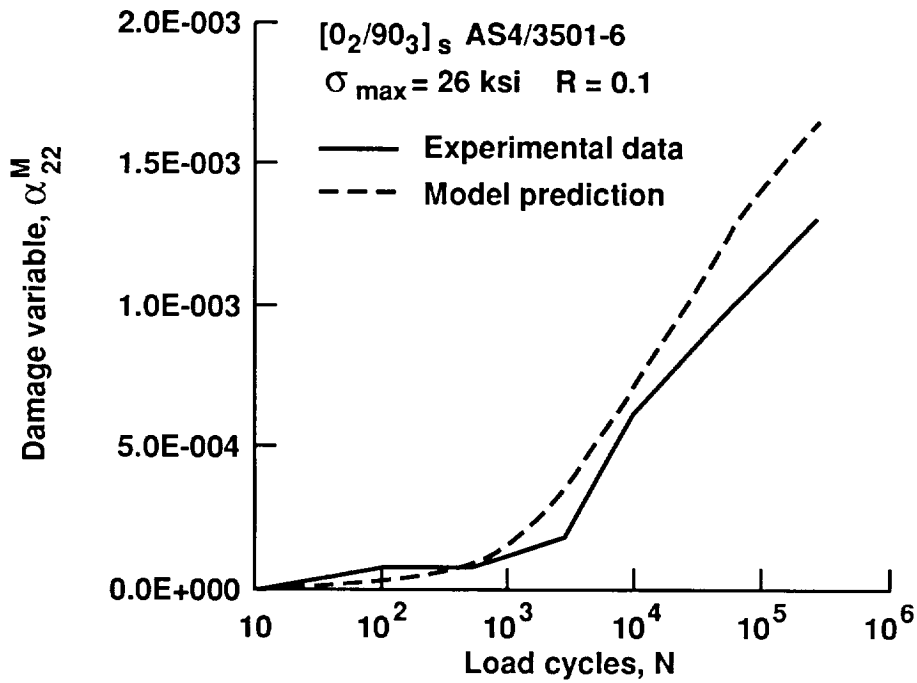
Figure 17. Matrix crack damage in the 90° plies of a $[0_2/90_3]_s$ laminate for a maximum applied laminate stress of 26 ksi and R = 0.1.
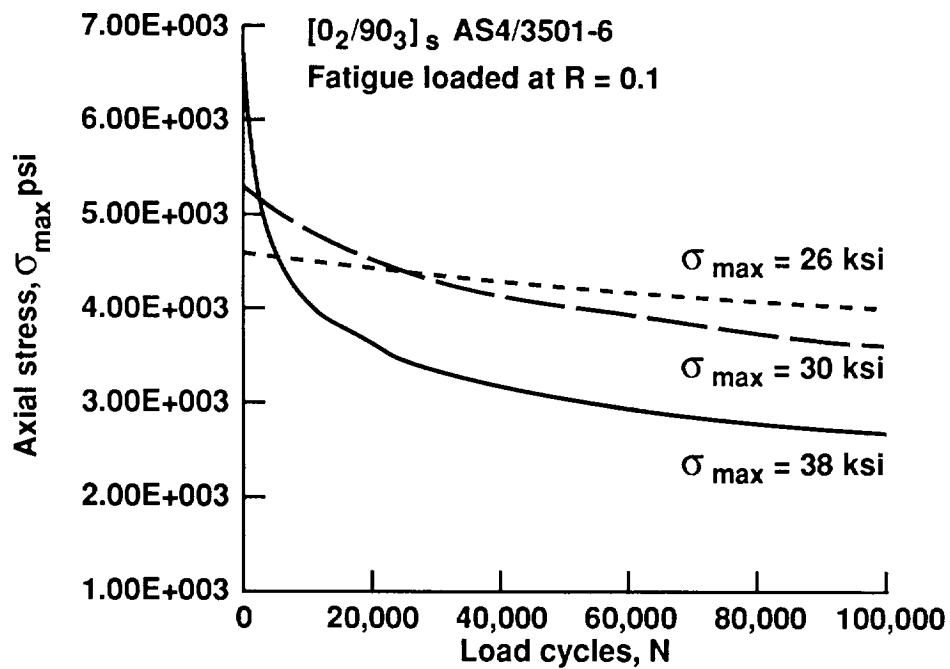

Figure 18. Damage-induced stress redistribution in the 90° plies of a $[0_2/90_3]_s$ laminate subjected to constant amplitude fatigue at R = 0.1.
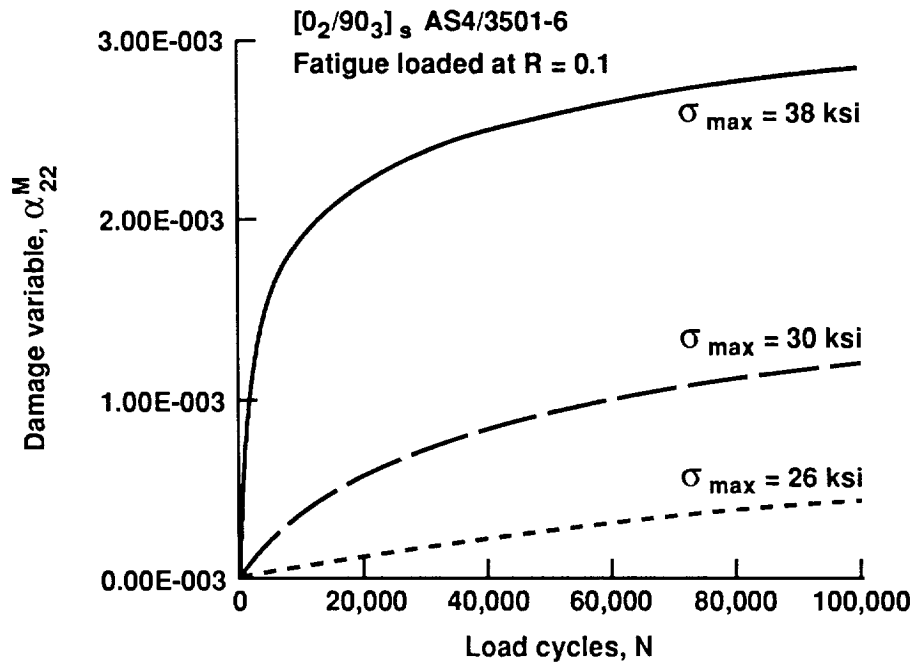
Figure 19. Evolution of damage ISV in the 90° plies of a $[0_2/90_3]_s$ laminate subjected to constant amplitude fatigue at R = 0.1.
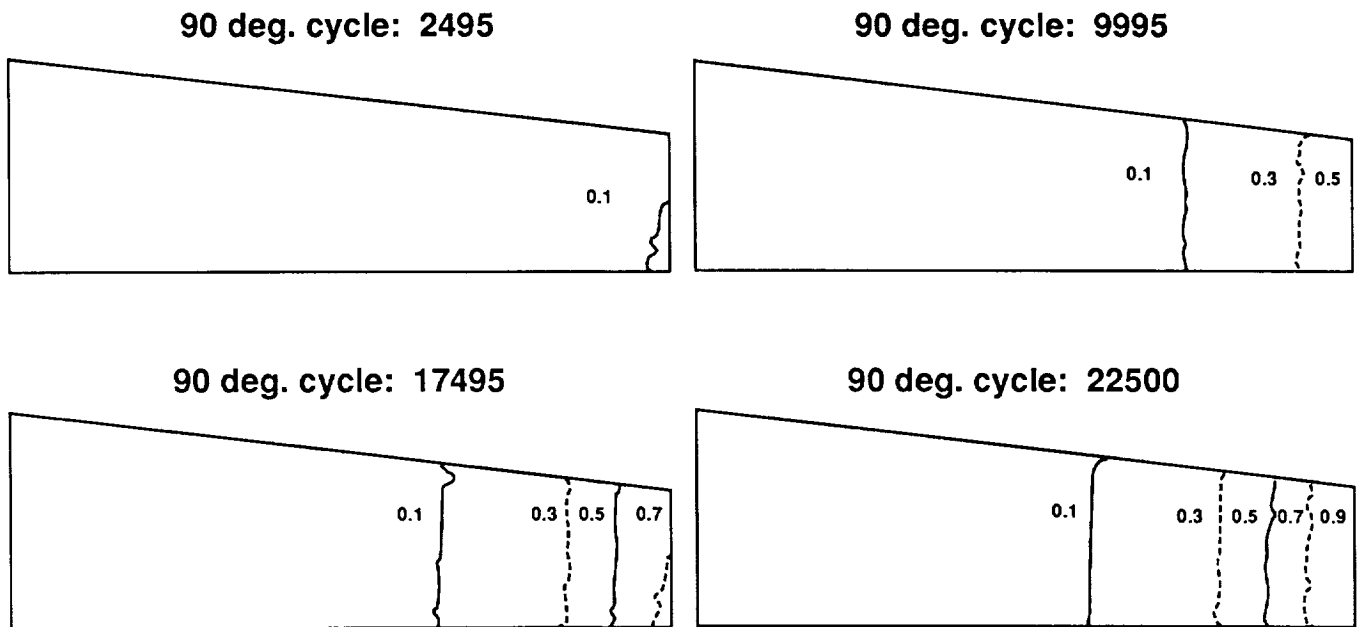

Figure 20. The accumulation of matrix cracks in the 90° plies during various points in the loading history.

0 deg. cycle: 2495

0 deg. cycle: 9995

0.1 0.3

0 deg. cycle: 17495

0.1 0.3

0 deg. cycle: 22500

0.1 0.3
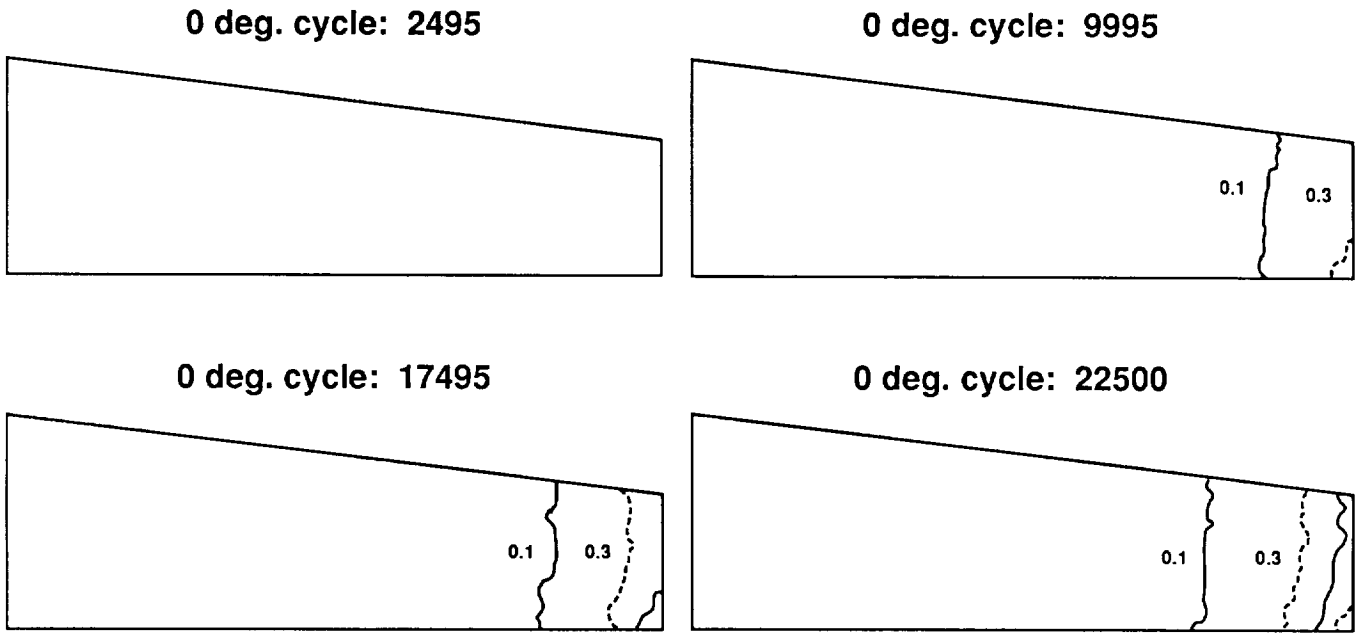
Figure 21. The accumulation of matrix cracks in the 0° plies during various points in the loading history.

Initial Material Condition

```
Foreign Object        NDI Limits      Curing and/or
Impact                                Environment
```

Current
Damage → Damage-Dependent → Effective Lamina
State   Laminate Analysis   and Laminate
                                  Stiffness Properties

Yes   Subcritical

Global
Structural   Current
Analysis   Applied
                Load

Increment Load   No   Progressive   Loading - History   Local Element
and Repeat Global ←   Damage   ← Dependent Damage   ← Material Level
Structural Analysis   Development   Growth Laws   Stress Analysis

Yes   Catastrophic

- Phenomenological
- Micromechanics
- Fracture Mechanics

Laminate Strength
and Life

Figure 22. Logic for laminate strength and life prediction methodology.